# A study of the $^{16}$O(e,e′p) reaction at deep missing energies

N. Liyanage,[17] B. D. Anderson,[13] K. A. Aniol,[2] L. Auerbach,[29] F. T. Baker,[7] E. J. Beise,[16] J. Berthot,[1] W. Bertozzi,[17] P. -Y. Bertin,[1] L. Bimbot,[22] W. U. Boeglin,[5] E. J. Brash,[24] V. Breton,[1] H. Breuer,[16] E. Burtin,[26] J. R. Calarco,[18] L. Cardman,[30] G. D. Cates,[23] C. Cavata,[26] C. C. Chang,[16] N. S. Chant,[16] J. -P. Chen,[30] E. Cisbani,[12] D. S. Dale,[14] A. Deur,[1] B. Diederich,[21] P. Djawotho,[33] B. Doyle,[14] J. -E. Ducret,[26] M. B. Epstein,[2] L. A. Ewell,[16] J. M. Finn,[33] K. G. Fissum,[17] H. Fonvieille,[1] B. Frois,[26] S. Frullani,[12] J. Gao,[17] F. Garibaldi,[12] A. Gasparian,[8,14] S. Gilad,[17] R. Gilman,[25] A. Glamazdin,[15] C. Glashausser,[25] J. Gomez,[30] V. Gorbenko,[15] T. Gorringe,[14] K. Griffioen,[33] F. W. Hersman,[18] R. Holmes,[28] M. Holtrop,[18] N. d'Hose,[26] C. Howell,[4] G. M. Huber,[24] C. E. Hyde-Wright,[21] M. Iodice,[12] C. W. de Jager,[30] S. Jaminion,[1] M. K. Jones,[33] K. Joo,[32] C. Jutier,[1,21] W. Kahl,[28] S. Kato,[34] J. J. Kelly,[16] S. Kerhoas,[26] M. Khandaker,[19] M. Khayat,[13] K. Kino,[31] W. Korsch,[14] L. Kramer,[5] K. S. Kumar,[23] G. Kumbartzki,[25] G. Laveissière,[1] R. De Leo,[10] A. Leone,[11] J. J. LeRose,[30] L. Levchuk,[15] M. Liang,[30] R. A. Lindgren,[32] G. J. Lolos,[24] R. W. Lourie,[27] R. Madey,[8,13,30] K. Maeda,[31] S. Malov,[25] D. M. Manley,[13] P. Markowitz,[5] D. J. Margaziotis[2] J. Marroncle,[26] J. Martino,[26] J. S. McCarthy,[32] K. McCormick,[21] J. McIntyre,[25] R. L. J. van der Meer,[24,30] Z. -E. Meziani,[29] R. Michaels,[30] J. Mougey,[3] S. Nanda,[30] D. Neyret,[26] E. A. J. M. Offermann,[30] Z. Papandreou,[24] C. F. Perdrisat,[33] R. Perrino,[11] G. G. Petratos,[13] S. Platchkov,[26] R. Pomatsalyuk,[15] D. L. Prout,[13] V. A. Punjabi,[19] T. Pussieux,[26] G. Quéméner,[33] R. D. Ransome,[25] O. Ravel,[1] Y. Roblin,[1] R. Roché,[6] O. A. Rondon-Aramayo,[32] P. G. Roos,[16] D. Rowntree,[17] G. Rutledge,[33] P. M. Rutt,[25] A. Saha,[30] T. Saito,[31] A. J. Sarty,[6] A. Serdarevic-Offermann,[24] T. P. Smith,[18] A. Soldi,[20] P. Sorokin,[15] P. Souder,[28] R. Suleiman,[13] J. A. Templon,[7] T. Terasawa,[31] L. Todor,[21] H. Tsubota,[31] H. Ueno,[34] P. E. Ulmer,[21] G. Urciuoli,[12] P. Vernin,[26] S. van Verst,[17] B. Vlahovic,[20] H. Voskanyan,[35] J. W. Watson,[13] L. B. Weinstein,[21] K. Wijesooriya,[33] R. Wilson,[9] B. Wojtsekhowski,[30] D. G. Zainea,[24] V. Zeps,[14] J. Zhao,[17] Z. -L. Zhou[17]

(The Jefferson Lab Hall A Collaboration)

[1] *Université Blaise Pascal/IN2P3, F-63177 Aubière, France*
[2] *California State University, Los Angeles, California 90032*
[3] *Institut des Sciences Nucléaires, F-38026 Grenoble, France*
[4] *Duke University, Durham, North Carolina 27706*
[5] *Florida International University, Miami, Florida 33199*
[6] *Florida State University, Tallahassee, Florida 32306*
[7] *University of Georgia, Athens, Georgia 30602*
[8] *Hampton University, Hampton, Virginia 23668*
[9] *Harvard University, Cambridge, Massachusetts 02138*
[10] *INFN, Sezione di Bari and University of Bari, I-70126 Bari, Italy*
[11] *INFN, Sezione di Lecce, I-73100 Lecce, Italy*
[12] *INFN, Sezione Sanitá and Istituto Superiore di Sanitá, Laboratorio di Fisica, I-00161 Rome, Italy*
[13] *Kent State University, Kent, Ohio 44242*
[14] *University of Kentucky, Lexington, Kentucky 40506*
[15] *Kharkov Institute of Physics and Technology, Kharkov 310108, Ukraine*
[16] *University of Maryland, College Park, Maryland 20742*
[17] *Massachusetts Institute of Technology, Cambridge, Massachusetts 02139*
[18] *University of New Hampshire, Durham, New Hampshire 03824*
[19] *Norfolk State University, Norfolk, Virginia 23504*
[20] *North Carolina Central University, Durham, North Carolina 27707*
[21] *Old Dominion University, Norfolk, Virginia 23529*
[22] *Institut de Physique Nucléaire, F-91406 Orsay, France*
[23] *Princeton University, Princeton, New Jersey 08544*
[24] *University of Regina, Regina, Saskatchewan, Canada, S4S 0A2*
[25] *Rutgers, The State University of New Jersey, Piscataway, New Jersey 08854*
[26] *CEA Saclay, F-91191 Gif-sur-Yvette, France*
[27] *State University of New York at Stony Brook, Stony Brook, New York 11794*
[28] *Syracuse University, Syracuse, New York 13244*
[29] *Temple University, Philadelphia, Pennsylvania 19122*
[30] *Thomas Jefferson National Accelerator Facilty, Newport News, Virginia 23606*
[31] *Tohoku University, Sendai 980, Japan*
[32] *University of Virginia, Charlottesville, Virginia 22901*
[33] *College of William and Mary, Williamsburg, Virginia 23187*
[34] *Yamagata University, Yamagata 990, Japan*
[35] *Yerevan Physics Institute, Yerevan 375036, Armenia*

(April 25, 2000)

The $^{16}$O(e,e′p) reaction was studied in quasielastic kinematics at $Q^2 = 0.8$ (GeV/c)$^2$ and $\omega = 439$ MeV. Cross sections and the $R_L$, $R_T$, and $R_{LT}$ response functions were extracted for missing energies between 25 MeV and 60 MeV and for missing momenta up to 355 MeV/c. For $E_{miss} < 50$ MeV and $P_{miss} < 150$ MeV/c, the results are generally explained by $1s_{1/2}$-state single-particle knockout. $R_L$ becomes small for $E_{miss} > 50$ MeV while $R_T$ remains substantial, indicating non-single-particle interactions. As $P_{miss}$ increases, the single-particle knockout calculations account for a decreasing fraction of the measured strength. Most of the continuum strength appears to reside in the $R_T$ and $R_{LT}$ responses.

PACS numbers: 25.30.Fj, 27.20.+n

The (e,e′p) reaction in quasielastic kinematics ($\omega \approx Q^2/2m_p$ where $Q$ and $\omega$ are the four-momentum and energy transfers) has long been a useful tool for the study of nuclear structure. (e,e′p) cross section measurements have provided both a wealth of information on the wave functions of protons inside the nucleus and stringent tests of nuclear theories. Response function measurements have provided detailed information about the different reaction mechanisms contributing to the cross section. These mechanisms include single- and multi-nucleon knockout, meson exchange currents (MEC), isobar excitations (IC), and final-state interactions.

In the first Born approximation, the unpolarized (e,e′p) cross section can be expressed as [1]

$$\frac{d^6\sigma}{d\Omega_e d\Omega_{p'} d\omega dE_{p'}} = \frac{p_{p'}E_{p'}}{(2\pi)^3}\sigma_{Mott}(V_L R_L + V_T R_T + V_{LT} R_{LT}\cos\phi + V_{TT} R_{TT}\cos 2\phi) \quad (1)$$

where $V_L, V_T, V_{LT}$, and $V_{TT}$ are kinematic factors dependent upon the electron vertex, $\phi$ is the angle between the electron scattering plane and the reaction plane, and $\sigma_{Mott}$ is the Mott cross section. $p_{p'}$ and $E_{p'}$ are the momentum and energy of the knocked-out proton, respectively. The four independent response functions $R_{\rm L}$ (longitudinal), $R_{\rm T}$ (transverse), $R_{\rm LT}$ (longitudinal-transverse), and $R_{\rm TT}$ (transverse-transverse) contain the information that can be extracted from the hadronic system using the (e,e′p) reaction.

In parallel kinematics $\vec{P}_{miss} \parallel \vec{q}$ ($\vec{P}_{miss} = \vec{p_{p'}} - \vec{q}$, where $\vec{q}$ is the three momentum transfer). Since the out-of-plane angle $\phi$ is not defined, only $R_L$ and $R_T$ survive in the expression for the cross section. Thus, the Rosenbluth method may be used to separate $R_L$ and $R_T$. In perpendicular kinematics all four terms are present in the expression. By measuring the cross section on both sides of $\vec{q}$ ($\phi = 0°$ and $\phi = 180°$) keeping all other kinematic variables constant, $R_{LT}$ can be extracted according to

$$R_{LT} = \frac{(2\pi)^3}{E'_p p'_p \sigma_{Mott}}\left[\frac{\sigma(0°) - \sigma(180°)}{2V_{LT}}\right] \quad (2)$$

An in-plane Rosenbluth separation in the case of perpendicular kinematics allows for the separation of $R_L + \frac{V_{TT}}{V_L}R_{TT}$ (hereafter referred to as $R_{L+TT}$) and $R_T$.

Originally, the quasielastic cross section was attributed entirely to single-particle knockout from the valence states of the nucleus. However, a series of $^{12}$C(e,e′p) single-particle knockout experiments performed at MIT-Bates [2–5] which sampled various kinematic regions measured much larger cross sections at high missing energy ($E_{miss} = \omega - T_p$ where $T_p$ is the final proton kinetic energy) than was expected by single particle knockout models. $^{12}$C(e,e′p) response function data reported by Ulmer *et al.* [2] show a substantial increase in the transverse-to-longitudinal difference above the two-particle emission threshold. This enhancement suggests the presence of an additional, transverse, non-single-particle reaction mechanism. $R_T/R_L$ enhancement above the two-nucleon emission threshold has also been observed at NIKHEF-K for $^6$Li [6] and $^{12}$C [7]. More recently, a Jefferson Lab Hall C experiment has observed $R_T/R_L$ enhancement above the two-nucleon emission threshold for $^{12}$C, $^{56}$C, and $^{197}$Au at $Q^2 = 0.6$ (GeV/c)$^2$ [10]. These findings suggest that a significant part of the cross section at large missing energies is due to two-body and multi-body processes.

There have been several theoretical attempts [11–13] to explain the continuum strength using two-body knockout models and final-state interactions, but no single model can explain all data. It has also been suggested that short-range and tensor correlations could play a major role in populating the high-$E_{miss}$ continuum. Müther *et al.* [14] have shown that these effects shift strength from conventional quasi-hole states to high-$E_{miss}$, high-$P_{miss}$ channels.

In this experiment [15], we measured the $^{16}$O(e,e′p) reaction in the quasielastic region at $Q^2 = 0.8$ (GeV/c)$^2$ and $\omega = 439$ MeV. We extracted the $R_L$, $R_T$, and $R_{LT}$ response functions from cross sections measured at several beam energies and electron angles for $E_{miss} < 60$ MeV and $P_{miss} < 355$ MeV/c. This was the first Jefferson Lab Hall A experiment and the first response function separation on a complex nucleus at large $E_{miss}$ and $P_{miss}$. This paper reports the results for $E_{miss} > 25$ MeV.

We scattered the continuous wave incident electron beam from a waterfall target [16] with three foils, each $\sim 130$mg/cm$^2$. We detected the scattered electrons and knocked-out protons in the High Resolution Spectrometers. The details of the Hall A experimental setup are given in [17,18].

We measured the $^{16}$O(e,e′p) cross section at three beam energies keeping $|\vec{q}|$ and $\omega$ fixed in order to separate response functions and understand systematic uncertainties (the kinematic variables of the measurements are given in Table I). For the $\theta_{pq} = \pm 8°$ setting, $R_{LT}$ values extracted at beam energies of 1.643 GeV and 2.442 GeV

agree well within statistical uncertainties. This indicates that the systematic uncertainties for the experiment are smaller than the statistical uncertainties.

The accuracy of a response function separation depends on precisely matching the values of $|\vec{q}|$ and $\omega$ for different kinematic settings. In order to match $|\vec{q}|$, we measured H(e,ep) (also using the waterfall target) with a pin-hole collimator in front of the HRS$_e$. The momentum of the detected protons was thus equal to $\vec{q}$. We determined the H(e,ep) momentum peak to $\frac{\delta p}{p} = 1.5 \times 10^{-4}$, allowing us to match $|\vec{q}|$ to $1.5 \times 10^{-4}$ between the different kinematic settings. Throughout the experiment, H(e,e) data, measured simultaneously with the $^{16}$O(e,e'p), provided a continuous monitor of both luminosity and beam energy.

The radiative corrections to the measured cross sections were performed using the code RADCOR [18,19], which unfolds the radiative tails in $E_{miss}/P_{miss}$ space. For the $\theta_{pq} = 0^\circ$ kinematic setting of this experiment, the H(e,ep) peak and the associated radiative tail were present in the coincidence phase space for $^{16}$O. To remove H(e,ep) events, we cut out all events with $P_{miss} < 45$ MeV/c.

We compared our results to single-particle knockout calculations by Kelly [20], and Ryckebusch [25–27] to determine how much of the observed continuum strength can be explained by $1s_{1/2}$-state knockout. Kelly [20] performed DWIA calculations using a relativized Schrödinger equation in which the dynamical enhancement of lower components of Dirac spinors is represented by an effective current operator. The NLSH model was used for bound-state wave functions and the EDAIO optical model was used for outgoing distorted waves. These calculations were previously shown to provide good fits to the p-shell missing momentum distributions up to 340 MeV/c [21]. Similar calculations were also made for the s-shell and spread over missing energy using a Lorentian parameterization [28]. Figure 1 shows that with a normalization factor of 0.73 this model provides a good description of the continuum data for small $p_m$, but that the direct s-shell cross section falls too rapidly with $p_m$ to describe the continuum data for large $p_m$. The $E_m$ distribution becomes nearly flat for $p_m > 250$ MeV/c, showing little evidence for significant s-shell strength. Relativistic DWIA calculations by other authors [22,23] show similar results.

Figure 1 also shows calculations by Ryckebusch *et al.* [25–27] using a nonrelativistic Hartree-Fock model. The Hartree-Fock model of single-nucleon knockout uses the same potential for both the ejectile and bound nucleons. Unlike DWIA, this approach conserves current at the one-body level, but it also requires much smaller normalization factors because it lacks a mechanism for diversion of flux from the single-nucleon knockout channel. Furthermore, the absence of an absorptive potential has a strong effect upon the missing momentum distribution. Figure 1 shows that the Hartree-Fock model, distributed over missing energy according to the same Lorentzian spreading function, produces much larger cross sections for $p_m > 250$ MeV/c than the DWIA model, for s-shell knockout. Although the Hartree-Fock model appears to provide a better description of the s-shell data for $p_m > 250$ MeV/c, it substantially overestimates the p-shell cross section (see table III), which is described well by DWIA. We have shown that the most important difference between these single-nucleon knockout models is the absorptive potential and that omission increases cross sections for $p_m \sim 300$ MeV/c by an order of magnitude for both p-shell and s-shell.

Also shown in the Figure 1 are (e,e'pn) and (e,e'pp) contributions calculated by Ryckebusch*et al* [29]. This calculation includes contributions mediated by pion-exchange currents, intermediate $\Delta$ creation and central and tensor short-range correlations.

For the $\langle P_{miss} \rangle = 50$ MeV case, the phase-space limitations prevented us from calculating cross sections for $E_{miss} > 80$ MeV. For the higher $P_{miss}$ settings the continuum cross section for $E_{miss} > 80$ MeV is almost flat in $E_{miss}$. Table II shows the averaged cross section for 80 MeV $< E_{miss} <$ 120 MeV for these three $P_{miss}$ settings. The reduction of the continuum cross section from $\langle P_{miss} \rangle = 145$ MeV to $\langle P_{miss} \rangle = 340$ MeV is roughly by a factor of 2. Compared to the rapid depletion of the valence shell cross section with increasing $P_{miss}$ as illustrated by the $1p_{1/2}$ shell cross sections measured during the same experiment [30], the continuum cross section can be regarded as almost flat in $P_{miss}$ as well. This is in qualitative agreement with the (e,e'pp) and (e,e'pn) calculations by Ryckebusch*et al* [29] who have shown the total (e,e'pn) and (e,e'pp) contribution to be fairly constant and of the order $1 \times 10^{-3}$nb/MeV$^2$/sr$^2$, for this $E_{miss}$ range. However this calculation accounts for only about half of the excess continuum strength.

Figure 1 exhibits a gradual filling of the 20MeV $\leq E_{miss} \leq$ 40 MeV missing-energy range with increasing $P_{miss}$. Effects of non-single particle origin would reflect themselves in the excitation of states with a complex structure in between the p- and s-shell. The filling up of this $E_{miss}$ range may be an indication of such behavior.

Figure 2 presents the separated response functions for the $\theta_{pq} = 0^\circ$ setting ($\langle P_{miss} \rangle \approx 60$ MeV/c). The wide peak centered around $E_{miss} \approx 40$ MeV in both $R_L$ and $R_T$ corresponds primarily to single-particle knockout from the $1s_{1/2}$-state. The difference between the transverse and longitudinal spectral functions $(S_T - S_L)$[1],

[1] $S_X = \frac{\sigma_M V_X R_X}{\sigma_X^{ep}}$, where X $\epsilon$ $\{T, L\}$, and $\sigma_X^{ep}$ is calculated

which is expected to be zero for a free nucleon, appears to be nonzero for $E_{miss} > 40$ MeV. While the magnitude of $(S_T - S_L)$ measured here is smaller than that measured by Ulmer *et al.* [2] at $Q^2 = 0.14$ (GeV/c)$^2$ and by Dutta *et al.* at $Q^2 = 0.6$ (GeV/c)$^2$, it is larger than $S_T - S_L$ measured by Dutta *et al.* at $Q^2 = 1.8$ (GeV/c)$^2$. This may suggest that at high $Q^2$ the single-particle mechanism is more promiment than at lower $Q^2$.

Figure 3 presents the separated response functions for $|\theta_{pq}| = 8^\circ$ setting ($\langle P_{miss} \rangle \approx 145$ MeV/c). The Mahaux parameterization does not reproduce the shape of $R_L$ or $R_T$ as a function of missing energy. For $E_{miss} < 35$ MeV, all calculated response functions underestimate the data. For $E_{miss} > 50$ MeV, $R_{L+TT}$ (which is mainly longitudinal because $\frac{V_{TT}}{V_L} R_{TT}$ is estimated to be only about 7% of $R_L$ [20]) is consistent with both zero and the calculations. $R_T$, on the other hand, appears to retain strength above 50 MeV. This is in agreement with the parallel kinematics results of the present experiment and also with the results from MIT-Bates and Hall C. $R_{LT}$ is about twice as large as all three calculations over the entire range of $E_{miss}$.

Figure 4 presents the separated response functions for the $|\theta_{pq}| = 16^\circ$, $\langle P_{miss} \rangle \approx 280$ MeV/c setting. At this setting $R_{L+TT}$ is close to zero as predicted by all three calculations. However, $R_T$ and $R_{LT}$ are much larger than the DWIA calculation and approximately as large as the HF calculation. Neither $R_T$ nor $R_{LT}$ shows a peak at $E_{miss} \approx 40$ MeV where single-particle knockout from the $1s_{1/2}$-state is expected.

In conclusion, the data at $\langle P_{miss} \rangle \approx 60$ MeV/c are consistent with previously reported $R_L/R_T$ behavior. While the magnitude of $(S_T - S_L)$ measured here is at $Q^2 = 0.6$ (GeV/c)$^2$ smaller than that measured priviously at lower momentum transfers it is larger than $S_T - S_L$ measured by Dutta *et al.* at $Q^2 = 1.8$ (GeV/c)$^2$. This data indicate the filling up of the $E_{miss}$ range between the p- and s-shells (20MeV $\leq E_{miss} m \leq 40$ MeV) above single particle calculations with increasing $P_{miss}$. This may be due to the excitation of complex states with non-single particle origin. While the cross section and the response functions measured at $P_{miss} < 75$ MeV/c are described well by the Lorentzian shape expected for the s-shell, the cross section measured at higher missing momenta does not exhibit any resemblance to the Lorentzian. This is a clear indication that the single particle contribution dicreases with increasing $P_{miss}$ as predicted by theory. However an almost flat continuum strength of the order of few times $10^{-3}$nb/MeV$^2$/sr$^2$ seem to persist to the highest measured $P_{miss}$ this is in qualitative agreement with the calculations of Janssen*et al* of the (e,e′pn) and (e,e′pp) contributions. However this calculation accounts for only about half of the excess continuum strength.

from the off-shell ep cross section obtained using deForest's cc1 prescription [8,9].


[1] J.J. Kelly, Adv. Nucl. Phys. **23**, ed. by J.W. Negele and E. Vogt, 75 (1996).
[2] P.E. Ulmer *et al.*, Phys. Rev. Lett. **59**, 2259 (1987).
[3] R. Lourie *et al.*, Phys. Rev. Lett. **56**, 2364 (1986).
[4] L. Weinstein *et al.*, Phys. Rev. Lett. **64**, 1646 (1990).
[5] J.H. Morrison, Phys. Rev. **C59**, 221 (1999).
[6] J.B.J.M. Lanen *et al.*, Phys. Rev. Lett. **64**, 2250 (1990).
[7] G. van der Steenhoven *et al.*, Nucl. Phys. **A480**, 547 (1988).
[8] T. de Forest, Nucl. Phys. A **392,** 232 (1983).
[9] T. de Forest, Ann. Phys **45**, 365 (1967).
[10] D. Dutta, Ph.D. thesis, Northwestern University, 1999 (unpublished).
[11] J. Ryckebusch *et al.*, Nucl. Phys. **A624**, 581 (1997).
[12] A. Gil *et al.*, Nucl. Phys. **A627**, 599 (1997).
[13] T. Takaki, Phys. Rev. **C39**, 359 (1989).
[14] H. Muther *et al.*, Phys. Rev. **C49**, R17 (1994).
[15] A. Saha, W. Bertozzi, R.W. Lourie, and L.B. Weinstein, Jefferson Laboratory Proposal 89-003, 1989; K.G. Fissum, MIT-LNS Internal Report #02, 1997.
[16] F. Garibaldi *et al.*, Nucl. Instrum. Methods **A314,** 1 (1992).
[17] www.jlab.org/Hall-A/equipment/HRS.html
[18] N. Liyanage, Ph.D. thesis, MIT, 1999 (unpublished).
[19] E. Quint, Ph.D. thesis, University of Amsterdam, 1988 (unpublished).
[20] J.J. Kelly, Phys. Rev. **C60**, 044609 (1999).
[21] J. Gao *et al.*, Phys. Rev. Lett. **84**, 3265 (2000).
[22] A. Picklesimer, J. W. van Orden, and S. J. Wallace, Phys. Rev. **C 32**, 1312 (1985).
[23] J. M. Udías, J. A. Caballero, E. M. de Guerra, J. E. Amaro, and T. W. Donnelly, Phys. Rev. Lett. **83**, 5451 (1999).
[24] M. Hedayati-Poor, J.I. Johansson, and H.S. Sherif, Phys. Rev. **C51**, 2044 (1995)
[25] J. Ryckebusch *et al.*, Nucl. Phys. **A476**, 237 (1988).
[26] J. Ryckebusch *et al.*, Nucl. Phys. **A503**, 694 (1989).
[27] V. Van der Sluys *et al.*, Phys. Rev. **C55** 1982 (1997).
[28] J.P. Jeukenne and C. Mahaux, Nucl. Phys. **A394**, 445 (1983).
[29] S. Janssen, J. Ryckebusch, D. Debruyne and W. Van Nespen, nucl-th/9911054, to be published in Nucl. Phys. **A**
[30] J. Gao, Ph.D. thesis, MIT, 1999 (unpublished).


| $E_{\rm beam}$ (GeV) | $\theta_e$ ($^\circ$) | $\theta_{pq}$ ($^\circ$) |
|---|---|---|
| 0.843 | 100.7 | 0, 8, 16 |
| 1.643 | 37.2 | 0, ±8 |
| 2.442 | 23.4 | 0, ±2.5, ±8, ±16, ±20 |

TABLE I. Experimental Kinematics

| $\lvert\langle P_{miss}\rangle$ MeV | $\langle\lvert\sigma\rangle_{80\ \mathrm{MeV}<E_{miss}<120\mathrm{MeV}}$ nb/MeV$^2$/sr$^2$ | $\langle\sigma\rangle_{1p1/2}$ nb/MeV/sr$^2$ |
|---|---|---|
| 145 | $3.8 \times 10^{-3} \pm 0.3 \times 10^{-3}$ | $1.183\pm$ |
| 280 | $2.8 \times 10^{-3} \pm 0.2 \times 10^{-3}$ | $2.23 \times 10^{-2}\pm$ |
| 340 | $1.7 \times 10^{-3} \pm 0.1 \times 10^{-3}$ | $3.98 \times 10^{-3}\pm$ |

TABLE II. Averaged continuum cross section compared to $1p_{1/2}$ cross section measured during this experiment

| $\langle P_{miss}\rangle$ MeV | $\sigma_{1p1/2}$ nb/MeV/sr$^2$ | $\sigma^{Ryckebusch}_{1p1/2}$ nb/MeV/sr$^2$ |
|---|---|---|
| -279 | $(3.028 \pm 0.287) \times 10^{-2}$ | $2.63 \times 10^{-1}$ |
| -149 | $1.461 \pm 0.026$ | 1.92 |
| -60 | $1.538 \pm 0.051$ | 2.72 |
| 60 | $1.598 \pm 0.046$ | 1.84 |
| 149 | $0.906 \pm 0.027$ | 1.97 |
| 279 | $(1.433 \pm 0.286) \times 10^{-2}$ | $4.35 \times 10^{-1}$ |

TABLE III. $1p_{1/2}$ cross section from this expeirment comapred to the HF impulse approximations calculations by Ryckebusch

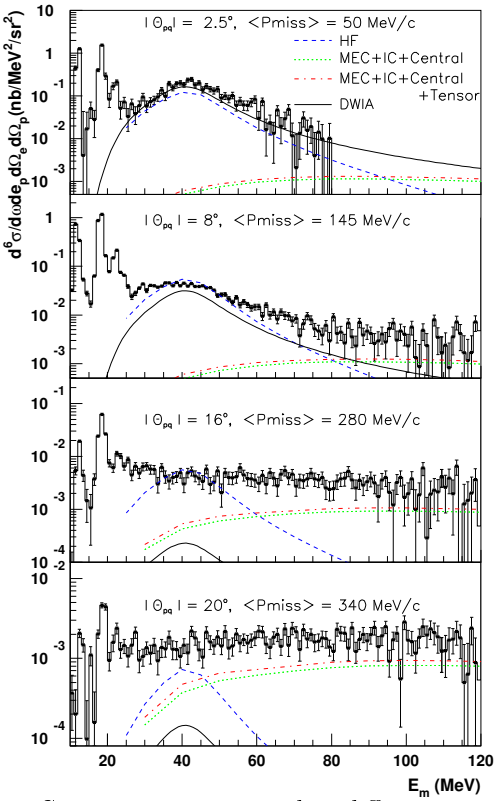


FIG. 1. Cross sections measured at different missing momenta as a function of missing energy. The curves show the $1s_{1/2}$-state single-particle strength calculated by Kelly folded with the Lorentzian parameterization of Mahaux.

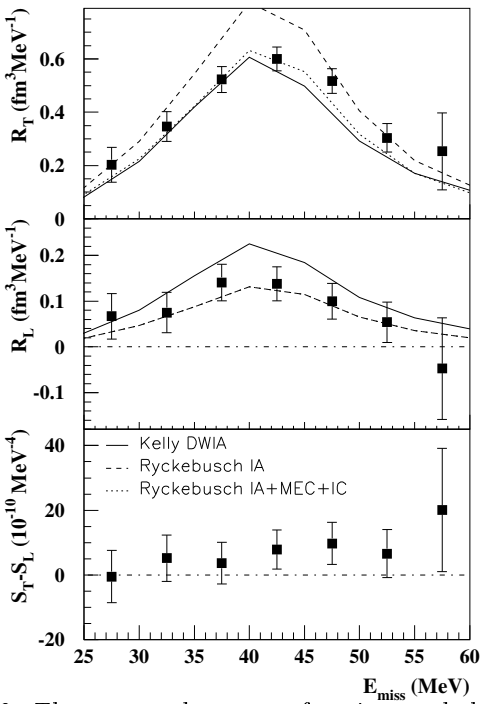


FIG. 2. The separated response functions and the difference of the longitudinal and transverse spectral functions for the $|\theta_{pq}| = 0°$ setting ($\langle P_{miss}\rangle \approx 60$ MeV/c). The calculations have been binned in the same manner as the data.

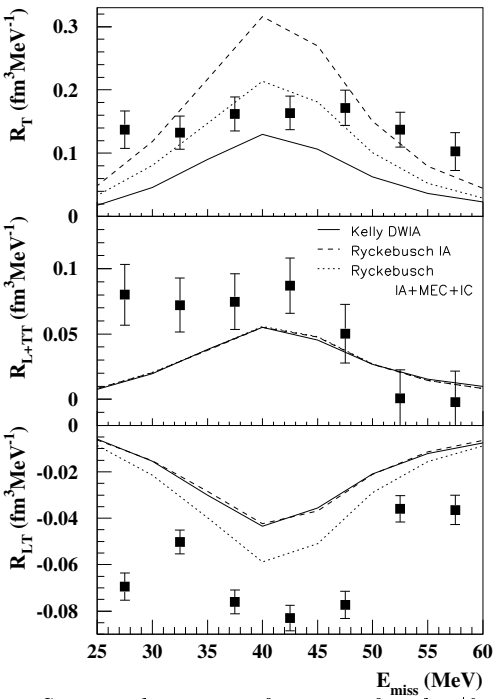


FIG. 3. Separated response functions for the $|\theta_{pq}| = 8°$ setting ($\langle P_{miss}\rangle^{average} \approx 145$ MeV/c). Plots show (from top to bottom): $R_{LT}$, $R_T$, and $R_{L+TT}$.

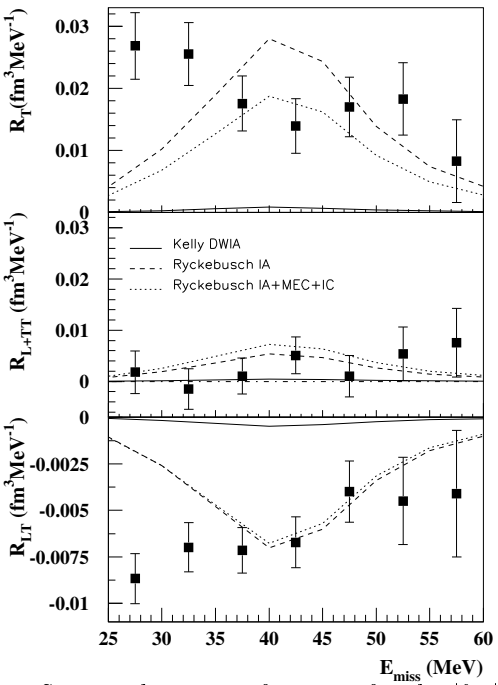


FIG. 4. Separated response functions for the $|\theta_{pq}| = 16°$ setting ($\langle P_{miss}\rangle \approx 280.0$ MeV/c). Plots show (from top to bottom): $R_{LT}$, $R_T$, and $R_{L+TT}$.